doi: 10.1209/0295-5075/98/34005

Salt crystallisation at the surface of a heterogeneous porous medium

Stephanie Veran-Tissoires, Manuel Marcoux and Marc Prat[(a)]

INPT, UPS, IMFT (Institut de Mécanique des Fluides de Toulouse), Université de Toulouse - Allée Camille Soula, F-31400 Toulouse, France, EU and
CNRS, IMFT - F-31400 Toulouse, France, EU

Abstract – Evaporation of saline solutions from a porous medium often leads to the precipitation of salt at the surface of the porous medium. It is commonly observed that the crystallized salt does not form everywhere at the porous medium surface but only at some specific locations. To explain this phenomenon, we consider efflorescence formation at the surface of a saturated heterogeneous porous column (finer porous medium in coarse porous medium background) in the wicking situation. We study the impact of permeability and porosity contrasts on the efflorescence formation location from a simple visualisation experiment and Darcy's scale numerical simulations. We show that the porosity is the most sensitive parameter for our experiment and that efflorescence forms at the surface of the medium of lower porosity. A simple efflorescence growth model is then used to explain why the efflorescence continues to grow at the surface of the lower porosity medium without spreading over the adjacent surface of the greater porosity medium.

Introduction. – Understanding of evaporation from porous media in the presence of dissolved salts is important in relation with several applications, such as soil physics [1] or the underground sequestration of CO_2 [2]. Another important field is the protection of buildings and of our cultural heritage [3] because of the severe damages caused by the salt crystallisation [4–6], that often results from the evaporation process. Depending on various factors such as the type of salt or the evaporation conditions [6], salt can precipitate within the porous medium where it forms subflorescence or at the surface of the porous medium where it forms efflorescence. The latter can be an important issue for the conservation of old paintings and frescoes [3]. Although the problem has motivated many studies, *e.g.*, [3–6] and references therein, owing to the significance of related practical issues, the understanding of the efflorescence formation and growth at the surface of a porous material is surprisingly not very advanced. As discussed in this paper, this is because efflorescence results from a series of complex coupled phenomena between the internal transport of salt within the underlying porous materials, the external evaporation and the non-equilibrium growth process associated with crystallisation. However, developing theories and modelling of efflorescence formation and growth (as a first step toward the still more involved problem of surface degradation) does not appear out of reach. The present paper is viewed as a step in this direction.

Even small samples of real porous media are rarely homogeneous at Darcy's scale and thus characterised by spatial variations in permeability and porosity. An archetypical example is a brick wall with properties markedly different in the bricks and the inter-brick mortar. The question thus arises as to whether the efflorescence will form at the surface of the bricks, of the mortar or both. To gain insight into the effect of structural heterogeneities on the location of the efflorescence formation and growth, we developed the simple experiment described in the next section.

Experiment. – The experimental set-up is sketched in fig. 1. Evaporation takes place at the top surface of the porous medium and the dissolved salt is transported across the sample to the evaporative surface from the reservoir in contact with the porous material at its bottom. As sketched in fig. 2, the experiment is performed for a homogeneous column (a pack of 1 mm glass beads) as well as for a heterogeneous one: a column containing a radially symmetric fine textured inclusion in the middle of a coarser porous medium. The coarser porous medium is the same as in the homogeneous column whereas the inclusion is a consolidated porous medium made of sintered glass

[(a)] E-mail: mprat@imft.fr

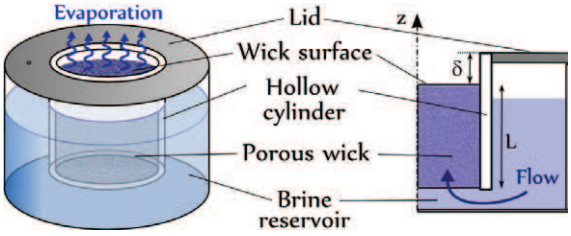

Fig. 1: (Colour on-line) Sketch of the experiment. A column of porous medium of height $L = 35$ mm is set in a hollow cylinder (38 mm in diameter and 50 mm in height). The bottom portion of the sample is submerged in a near saturated aqueous solution of sodium chloride ($C = C_0 = 25\,\mathrm{g}$ NaCl/100 g solution; the saturation concentration is $C_{sat} = 26.4\,\mathrm{g}$ NaCl/100 g solution). The aqueous solution level in the brine reservoir is such that the medium remains saturated during the experiment duration owing to capillary rise. The system is set in a cylindrical enclosure (not shown) of controlled relative humidity ($RH \approx 7\%$) and temperature ($T \approx 22.4\,^\circ$C) (see [7] for more details). The distance δ between the porous medium surface and the cylinder entrance rim is 15 mm.

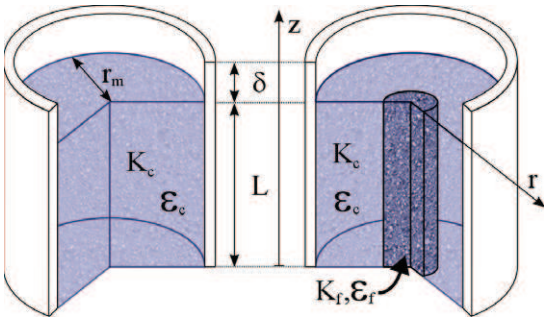

Fig. 2: (Colour on-line) The experiment is performed for a homogeneous porous column (left) as well as for a heterogeneous one (right).

beads of smaller diameter ($\approx 210\,\mu$m). Both the porosity and the permeability are smaller in the finer medium ($\varepsilon_f \approx 0.365$; $K_f = 7.16 \cdot 10^{-11}\,\mathrm{m}^2$) compared to the coarser medium ($\varepsilon_c \approx 0.39$; $K_c = 9.95 \cdot 10^{-10}\,\mathrm{m}^2$), see [8] for details on how these data have been obtained.

It is important to note that the sole difference between the two experiments lies in the sample (homogeneous *vs.* heterogeneous). All other parameters (evaporation rate at $t = 0$, initial salt concentration, salt concentration in the reservoir, sample dimensions, temperature and relative humidity in enclosure, etc.) are the same in both experiments.

The results are shown in fig. 3. As can be seen, the efflorescence forms and grows at the top of the central finer inclusion with the heterogeneous wick. By contrast, the efflorescence forms at discrete locations when the sample is homogeneous, not concentrated in the middle of the surface. The fact that efflorescence forms at discrete points at the surface of a homogeneous porous medium is discussed elsewhere [7,8]. Here we focus on the striking effect of large-scale (Darcy's scale) heterogeneity.

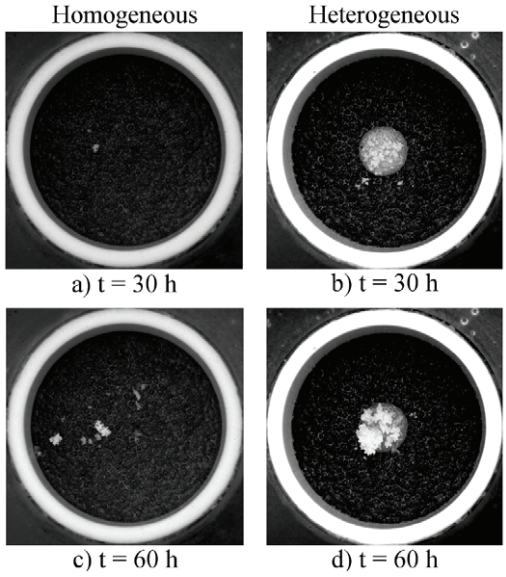

Fig. 3: Efflorescence formation (top view of sample surface). The top surface of the middle finer column of the heterogeneous wick is clearly visible in the images on the right. The white spots are efflorescence. As can be seen, efflorescence forms and grows at the surface of the finer porous material when the porous column is heterogeneous.

Discussion. – To explain the result shown in fig. 3, it is essential to note that the evaporation process induces a flow within the porous medium. Since the medium remains saturated, this means that the evaporation flux j at any point of the surface is balanced by a liquid flow (due to capillarity) of vertical Darcy velocity component v_z toward the considered point,

$$v_z = j/\rho_\ell, \tag{1}$$

where ρ_ℓ is the liquid density. As a result there exists a velocity field $\mathbf{v}$ within the porous wick directed on average toward the evaporative surface where a salt peak builds up and a salt concentration profile develops owing to the transport of the ions by advection. But as soon as a concentration gradient develops, diffusion tends to level off the accumulation. The competition between advection, which transports ions to the top of the sample and thereby causes accumulation, and diffusion, which tends to uniformise the concentration field is usually characterized by the Péclet number $Pe = \frac{uL}{D_s^*}$ [9–11], where D_s^* is the effective diffusion coefficient for the dissolved salt and the velocity u represents a characteristic interstitial velocity of the salt solution in the porous medium. A natural choice is $u = \mathbf{v}_z/\varepsilon \approx J/A/\rho_\ell/\varepsilon$ (J is the overall evaporation rate, A the top surface area, and ε the porosity of the porous medium). For our experiments, this gives $Pe \approx 1.5$ (with $D_s^* \approx 0.66\,D_s$ [12] where $D_s = 1.3 \cdot 10^{-9}\,\mathrm{m}^2/\mathrm{s}$ is the salt diffusion coefficient and $\varepsilon \approx 0.39$).

As a result of the significant advection, the ion distribution is uniform over most of the sample height. The concentration gradient is significant only in a narrow region of high salt concentration adjacent to the porous

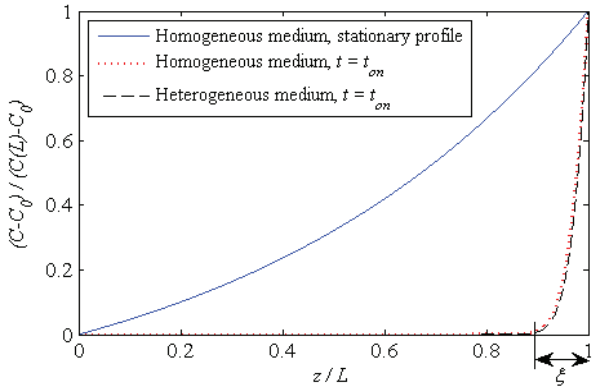

Fig. 4: (Colour on-line) Reduced salt concentration profiles (along the boundary between the fine and coarse porous media; the profiles are quite similar along any other vertical line within the sample) at the onset of efflorescence ($t = t_{on}$). The steady-state solution (see text) is also shown.

medium surface [9–11]. The size of this region increases with time but remains narrow (a few millimetres as discussed below). This explains why the salt crystallisation is observed at the porous medium surface and not inside the porous medium. Crystallisation occurs when the concentration reaches the saturation concentration C_{sat} (supersaturation effects are negligible for NaCl [13]), and C_{sat} is first reached at the sample surface owing to the advection effect (see fig. 4).

In-plane concentration spatial variations. To explain now the location of efflorescence formation at the surface of a finer porous medium in fig. 3, let us consider the equations governing the dissolved salt transport in the porous wick [9–11]:

$$\varepsilon \frac{\partial C}{\partial t} + \mathbf{v} \cdot \nabla C = \nabla \cdot (\varepsilon D_s^* \nabla C), \tag{2}$$

$$C = C_0, \quad \text{at } z = 0; \tag{3}$$

$$(C\mathbf{v} - \varepsilon D_s^* \nabla C) \cdot \mathbf{n}_z = 0, \quad \text{at } z = L. \tag{4}$$

The zero flux boundary condition (4), where $\mathbf{n}_z$ is the unit vector normal to the porous surface, means that the dissolved salt cannot leave the porous medium before the onset of crystallisation. Owing to the significance of advection, problem (2)–(4) clearly shows that it is crucial to understand the structure of the velocity field generated in the porous column to understand the concentration field structure.

The boundary value problem describing flow in the porous medium is given by (after decomposition of the pressure according to $P = P_{vis} + \rho_\ell g z$)

$$\nabla \cdot \mathbf{v} = 0, \tag{5}$$

$$\mathbf{v} = -\frac{K}{\mu} \nabla P_{vis}, \tag{6}$$

with the boundary conditions: $P_{vis} = P_0$ (arbitrary constant) at $z = 0$, $\mathbf{v} \cdot \mathbf{n}_r = 0$ on the porous column lateral side ($\mathbf{n}_r$ is the unit vector normal to the inner surface of the cylinder containing the porous medium) and eq. (1) at $z = L$ (wick top surface).

From the above equations, there are two obvious possible sources of velocity heterogeneities. The first one is the possible heterogeneity of the evaporation flux at the surface [7,8] since eq. (1) clearly indicates that heterogeneities in the evaporation flux induce heterogeneities in the velocity field within the porous medium (at least in the upper region of the sample). As discussed in [7], the evaporation flux distribution at the porous medium surface depends on the distance δ between the porous medium surface and the entrance rim of the hollow cylinder containing the porous medium (see fig. 1 and fig. 2). The evaporation flux is greater at the periphery of the surface for a sufficiently small δ, whereas the evaporation flux becomes constant over the surface for a sufficiently large δ. According to the results reported in [7], the evaporation flux can be considered as constant all over the porous surface for $\delta = 15\,\text{mm}$, which is the value of δ in the experiments leading to the results shown in fig. 3. The evaporation rate is measured from weighing the set-up [7] and this gives $J = 2 \cdot 10^{-8}\,\text{kg/s}$ and therefore $j = J/A = 1.76 \cdot 10^{-5}\,\text{kg/m}^2\text{/s}$.

The porous medium heterogeneities represent the other source of velocity heterogeneities. It is clear from eqs. (5), (6) and associated boundary conditions that the velocity field $\mathbf{v}$ can vary spatially even with a spatially uniform evaporation flux at the surface, *i.e.* a uniform filtration velocity at the surface (see eq. (1)) when the permeability varies spatially. Substituting eq. (6) into eq. (5) leads to the equation $K \Delta P_{vis} + \nabla K \cdot \nabla P_{vis} = 0$, which explicitly shows the dependence of the pressure field (and therefore of the velocity field according to eq. (6)) on any spatial variation in the permeability. However, to explain the result shown in fig. 3, it is crucial to note from eq. (2) that spatial variations not only in the permeability but also in the porosity can induce spatial variations in the salt concentration. The latter can also be induced by spatial fluctuations of the effective diffusion coefficient D_s^*. However, the effective diffusion coefficient can be related to porosity in the case of packings of spherical particles, $D_s^* \approx \varepsilon^{0.4} D_s$ [12]. Finally the two heterogeneity factors that affect the concentration field in the case of our experiment are thus the porosity and the permeability.

The occurrence of efflorescence at the surface of the central finer column can then be qualitatively explained. Firstly, the smaller porosity (0.365 compared to 0.39 in the coarse porous medium) induces a higher interstitial velocity $\mathbf{u}_z$ at the surface of the central column (according to eq. (1), $\mathbf{u}_z = v_z/\varepsilon = j/\rho_\ell/\varepsilon$ at $z = L$), thus a locally greater advection effect. Secondly the average pressure drop in each column can be roughly estimated as $\delta P_{vis} \approx O(\frac{\mu \mathbf{v}_z L}{K}) \approx O(\frac{\mu j L}{K \rho_\ell})$ according to eqs. (6) and (1); thus it is greater in the finer central region owing to its lower permeability. As a result, the pressure P_f in the upper

region of the finer column is lower than the pressure P_c in the upper region of the coarser column ($P_f(L) < P_c(L)$). As a consequence, there should exist a flow directed from the coarser column toward the central finer column in the upper layer of the porous system directing the salt toward the central column. These two effects should explain the preferential onset of efflorescence at the surface of the central column. This qualitative analysis is supported by the numerical simulations presented in the next section.

Numerical simulations. – The transient transport problem represented by eqs. (2)–(4) together with eqs. (5), (6) and the associated boundary conditions is expressed in cylindrical coordinates and solved numerically using the commercial simulation software COMSOL Multiphysics for a spatially uniform initial concentration ($C = C_0$ throughout the sample at $t = 0$). The normal velocity at the surface is spatially uniform and imposed using eq. (1) (with $\rho_\ell = 1212\,\mathrm{kg/m^3}$ and $j = 1.76 \cdot 10^{-5}\,\mathrm{kg/m^2/s}$).

The numerical simulation first permits an estimate of the characteristic size ξ of the region of high salt concentration gradients adjacent to the evaporative surface. An upper bound ξ_{ub} to this size is given by the steady-state solution to eqs. (2)–(4) for the homogeneous case, which reads $C(z) = C_0 \exp(Pe\, z/L)$ and leads to $\xi_{ub} \approx L/Pe$. Since we start with a high initial salt concentration, the saturation concentration C_{sat} is reached during the transient evolution of the concentration in our experiment. As a result, the size ξ is much lower than ξ_{ub} when the saturation concentration is reached at the surface. As shown in fig. 4, this characteristic size $\xi(t)$ is found to be on the order of 3 mm at the onset of efflorescence formation. As expected [9–11], the salt concentration gradient is found to be essentially zero in the region $0 \leqslant z \leqslant L - \xi(t)$. Note that this holds for both the homogeneous and heterogeneous columns.

As depicted in fig. 5a), the filtration velocity $\mathbf{v}$ is, as expected, greater in the column of greater permeability and the flow from the coarser column to the finer column is clearly visible in the upper region (by contrast, the filtration velocity is uniform all over the porous sample in the homogeneous case). Thus, as depicted in fig. 5a), the salt is preferentially transported within the region of greater permeability over most of the column height and then redirected toward the lower permeability region in the top region of the porous column. The effective length L_{eff} of salt transport up to the surface of finer medium is therefore greater than L, leading to an effective Péclet number $Pe_{eff} \approx \frac{uL_{eff}}{D_s^*}$ greater than the Péclet number $Pe = \frac{uL}{D_s^*}$ associated with the transport up to the coarse-porous-medium surface, and thus to greater salt concentrations at the surface of the finer porous medium.

As shown in fig. 5b), the numerical parametric study leads to the following conclusion for the spatially uniform evaporation flux at the surface considered in this letter: 1) when the porosity is the same in the two columns, the saturation concentration is first reached at the surface

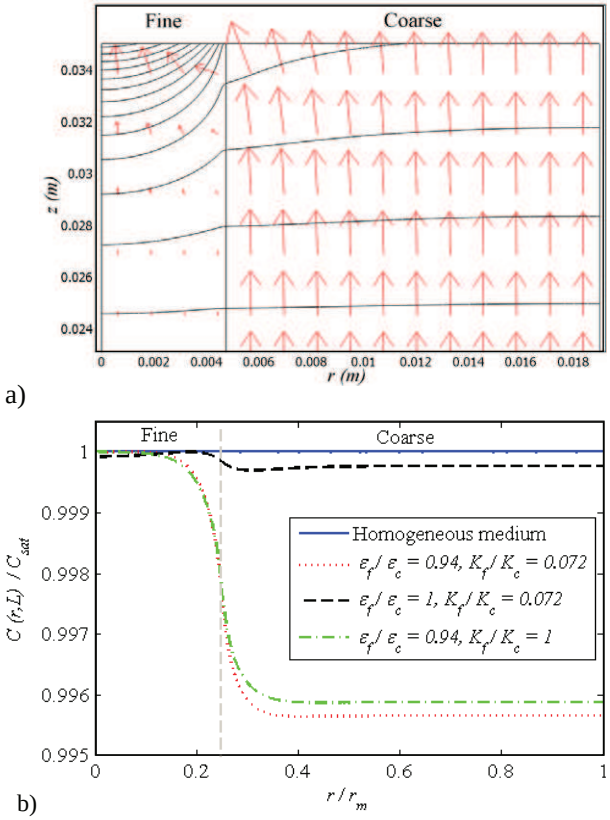

Fig. 5: (Colour on-line) a) Detail of the filtration velocity field in the top region of the heterogeneous sample (the black lines are isopressure lines). The values of parameters and the spatial dimensions are those of the experiment ($\varepsilon_f/\varepsilon_c = 0.94$, $K_f/K_c = 0.072$). As stated in the text, a uniform evaporation flux is imposed at the surface. b) Salt concentration at the surface of the porous wick as a function of radial coordinate r when the saturation concentration is reached (efflorescence onset).

of the lower-permeability column; 2) when the permeability is the same in the two columns, the saturation concentration is first reached at the surface of the lower-porosity column. In our experiment, the porosity contrast is $\varepsilon_f/\varepsilon_c \approx 0.94$, whereas the permeability contrast is $K_f/K_c \approx 0.072$. As shown in fig. 5b), both effects, namely the porosity and the permeability contrasts, contribute to the onset of efflorescence at the surface of the central region. However, fig. 5b) shows that the porosity contrast is the dominant effect in our experiment.

Structural heterogeneity superficial effect. – To gain further insight into the effect of Darcy's scale heterogeneities, it is important to note that the salt concentration gradients are significant only in the narrow top zone of thickness ξ (fig. 4). Since the salt concentration is uniform for $z < L - \xi$, this suggests that the porous medium heterogeneities have an impact on the efflorescence localisation only when present in the salt concentration gradient zone. To illustrate this, we have first performed numerical simulations of salt transport for finer central columns too short to reach the porous-medium surface. As depicted

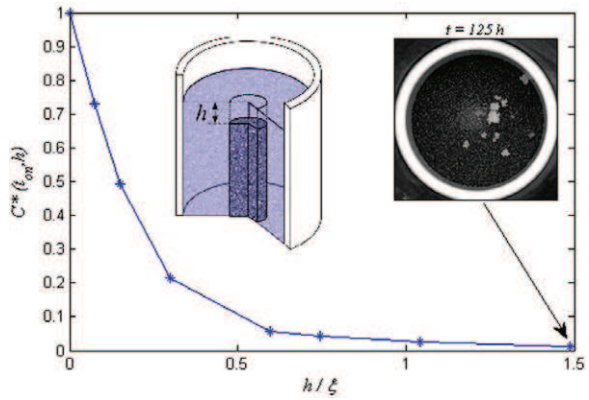

Fig. 6: (Colour on-line) Evolution of the concentration heterogeneity factor C^* at the surface of the porous medium at the onset of efflorescence ($t = t_{on}$) computed numerically as a function of the top-homogeneous-layer thickness h; $C^*(t_{on}, h) = \frac{C_{max}(t_{on},h) - C_{min}(t_{on},h)}{C_{max}(t_{on},0) - C_{min}(t_{on},0)}$, where C_{max} and C_{min} are the maximum and minimum concentrations at the surface, respectively. Shown in the right insert is the visualisation of efflorescence distribution obtained in an experiment performed with $h \approx 5\,\mathrm{mm}$.

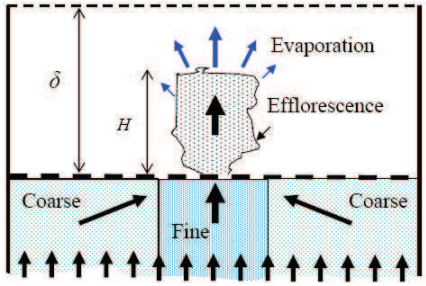

Fig. 7: (Colour on-line) The salt structure at the surface is porous and pumps by capillarity the liquid solution travelling in the underlying porous medium [14]. The structure grows owing to the salt deposition occurring preferentially at its top where evaporation is faster. As a result of efflorescence growth, evaporation from adjacent surface pores free from efflorescence is screened (the evaporation rate from those pores becomes smaller and smaller). By contrast, the liquid flow rate in surface pores in contact with the salt structure increases. As a result the crystallisation concentration is not reached in the screened pores. This induces a reorganization of the liquid solution flow structure within the upper layer of the porous medium, which explains why no efflorescence appears at the surface of the coarse porous medium, at least during the duration of our experiment.

in fig. 6, the system is formed in this case by a heterogeneous column of height $L - h$, surmounted by a homogeneous column of height h of coarse material. Except for its length, the properties of the buried heterogeneous column are the same as the ones corresponding to the experiment. The properties of the top homogeneous layer are those of the coarse material (packing of 1 mm spherical beads). As shown in fig. 6, the presence of heterogeneity has no effect on the salt distribution at the sample surface, as long as the thickness of the homogeneous top region is on the order of or greater than ξ. This has also been confirmed by an experiment performed with a heterogeneous column buried at a distance $h \approx 5\,\mathrm{mm}$ from the top surface, which corresponds to $h \approx 1.5\,\xi$, using for ξ the value estimated previously (fig. 4). The result is shown in fig. 6. As expected, the distribution of efflorescence is clearly quite similar to the one observed for the homogeneous column in fig. 3, without the preferential location in the middle region anymore, which characterises the heterogeneous column in fig. 3.

Efflorescence growth. – The key role played by advection effects explains the preferential onset of efflorescence at the surface of the inner column. Two puzzling questions remain, however. The efflorescence depicted in fig. 3d) (heterogeneous medium) is clearly at the surface of the inner finer column but has significantly grown since the occurrence of the first crystals. A first question is why the efflorescence continues to grow at the surface of the inner column without spreading over the surface of the coarser porous medium and without the occurrence of separated efflorescence structures at the surface of the coarse column. It can be even noted from the comparison between figs. 3b) and d) that the small efflorescence structures visible at the surface of the coarser column in fig. 3b) have disappeared in fig. 3d), that is when the efflorescence has sufficiently grown at the surface of the inner column. This fact raises the second question. To tentatively explain these phenomena it is crucial to note that the salt structures forming efflorescence are porous [14]. Evaporation takes place at the outer surface of an efflorescence structure, which consequently pumps by capillarity the aqueous solution contained in the underlying porous material. Hence, as sketched in fig. 7, the efflorescence structure first acts as a sink at the porous surface (the dissolved salt is directed toward the efflorescence). The second effect is a screening effect, *i.e.* the fact that the evaporation flux decreases in the regions of surface free of efflorescence. The detailed simulation of these coupled phenomena implies to model the efflorescence growth, the evolution of velocity and salt concentration fields within the underlying porous medium and the growing efflorescence structures. This is out of the scope of the present paper. We simply propose hereafter to illustrate in part the phenomenological explanations summarised in fig. 7.

The efflorescence structure is represented as a porous cylinder of constant diameter (the diameter of the inner fine medium) and growing height H (see fig. 8a)). Since the characteristic time of vapour diffusion (which is the dominant vapour transport mechanism from the efflorescence) $t_D \approx H^2/D$ (where $D \approx 2.5 \cdot 10^{-5}\,\mathrm{m^2/s}$ is the diffusion coefficient of water vapour in air) is very small ($t_D \approx 1\,\mathrm{s}$ for $H = 1\,\mathrm{cm}$) compared to the duration of efflorescence growth ($\sim 3 \cdot 10^5\,\mathrm{s}$ in the experiment), the evaporation from the efflorescence and at the surface of coarse porous medium (assumed free of efflorescence) can be computed assuming a quasi-steady purely diffusive transport of the water vapour, *i.e.* $\Delta p_v = 0$, where Δ is the

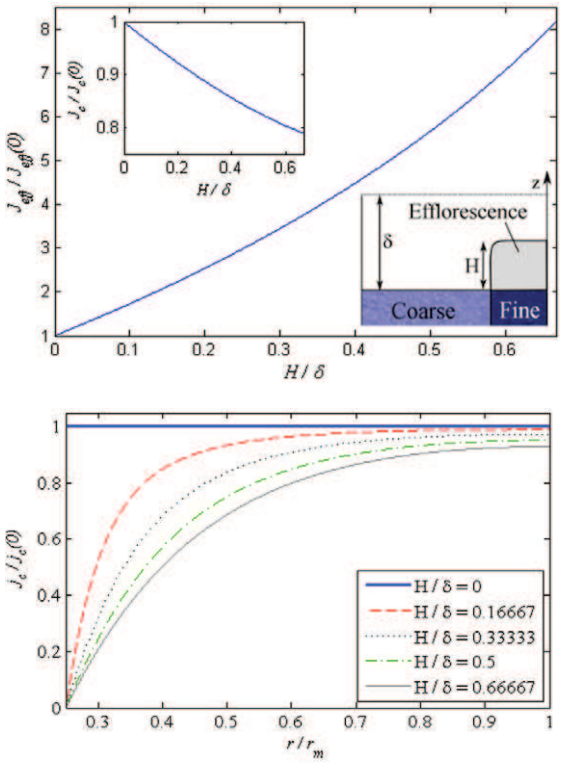

Fig. 8: (Colour on-line) Top: evolution of the total evaporation rate J_{eff} from the efflorescence structure as a function of efflorescence height H ($J_{eff}(0)$ is the evaporation rate from the finer porous medium at the onset of efflorescence growth). Shown in the insert is the evolution of the evaporation rate J_c at the surface of the coarser-porous-medium surface, which is free from efflorescence. Bottom: evolution of the evaporation flux $j_c(r, H)$ at the surface of the coarser-porous-medium surface.

Laplacian operator and p_v the water vapour partial pressure. Hence, we solve numerically (using again the software COMSOL Multiphysics) this equation expressed in cylindrical coordinates in the gas region with the boundary condition $p_v \approx 1170\,\mathrm{Pa}$ at $z = L + \delta$ (this gives an evaporation rate comparable to the measured value), $p_v = p_{ve}$ at $z = L$ (porous medium surface) and at the efflorescence surface (which at the efflorescence onset is formed by the fine porous medium surface); p_{ve} is the equilibrium vapour pressure ($p_{ve} \approx 0.75\, p_{vsat}$ for a saturated NaCl solution, where p_{vsat} is the saturation vapour pressure for pure water, $p_{vsat} \approx 2700\,\mathrm{Pa}$ at $T = 22.4\,^\circ\mathrm{C}$).

This gives the result plotted in fig. 8, which shows the increase of evaporation rate from the efflorescence and its decrease from the coarser porous medium surface as the efflorescence grows. Note also the distribution of the evaporation flux at the coarser porous medium surface, which decreases and becomes increasingly non-uniform. These evolutions together with the capillary pumping effect contribute to explain the dissolution phenomenon observed in the experiment and why no efflorescence forms at the surface of the coarse porous medium. In brief, it is surmised that the feedback effect due to the efflorescence growth has a strong impact on the salt concentration evolution in the top region of the porous medium, inducing a decrease in the concentration in the screened surface pores (and thus the dissolution of structures formed at earlier stages).

Conclusion. – Combined with the results reported in [9], the present paper clarifies the factors controlling the localisation of efflorescence at the evaporative surface of a saturated wick: the spatial variations in the evaporation flux at the surface [7] and the porous medium structural heterogeneities, namely the porosity and permeability spatial variations, as shown in the present paper. Both factors affect the velocity field in the region adjacent to the evaporation surface, where the salt concentration gradients are important owing to the generally dominant advection effect on the dissolved salt transport.

A simple efflorescence growth model has been presented to qualitatively explain the experimental observations after the onset of first crystals (such as the dissolution of efflorescence structures formed at earlier stages of efflorescence development, or the fact that the efflorescence continues to grow preferentially at the surface of the finer porous medium). These are explained by the change in the salt concentration induced by the efflorescence growth in relation with the porous nature of efflorescence, which acts as a capillary pump and contributes to the screening of evaporation from surface pores free of efflorescence around the efflorescence growing structure. The quantitative theory of efflorescence formation and growth is yet to come but we believe that the results presented here and in [7] open up the route in this direction.

REFERENCES

[1] Nassar I. N. and Horton R., *Soil Sci. Soc. Am. J.*, **63** (1999) 752.
[2] Peysson Y., Bazin B., Magnier C., Kohler E. and Youssef S., *Energy Procedia*, **4** (2011) 4387.
[3] Goudie A. and Viles H., *Salt Weathering Hazard* (Wiley London) 1997.
[4] Scherer G. W., *Cem. Concr. Res.*, **34** (2004) 1613.
[5] Shahidzadeh-Bonn N., Desarnaud J., Bertrand F., Chateau X. and Bonn D., *Phys. Rev. E*, **81** (2010) 066110.
[6] Rodriguez-Navarro C. and Doehne E., *Earth Surf. Processes Landf.*, **24** (1999) 191.
[7] Veran-Tissoires S., Marcoux M. and Prat M., *Phys. Rev. Lett.*, **108** (2012) 054502.
[8] Veran-Tissoires S., INPT PhD Thesis (2011).
[9] Puyate Y. T., Lawrence C. J., Buenfeld N. R. and Mcloughlin I. M., *Phys. Fluids*, **10** (1998) 566.
[10] Huinink H. P., Pel L. and Michels M. A. J., *Phys. Fluids*, **14** (2002) 1389.
[11] Guglielmini L., Gontcharov A., Aldykiewicz A. J. jr. and Stone H. A., *Phys. Fluids*, **20** (2008) 077101.
[12] Kim J. H., Ochoa J. A. and Whitaker S., *Transp. Porous Media*, **2** (1987) 327.
[13] Chatterji S., *Cem. Concr. Res.*, **30** (2000) 669.
[14] Sghaier N. and Prat M., *Transp. Porous Media*, **80** (2009) 441.